

A Simple and Efficient Absorption Filter for Single Photons from a Cold Atom Quantum Memory

Daniel T. Stack, Patricia J. Lee, and Qudsia Quraishi

Quantum Sciences Group, Army Research Laboratory, Adelphi, Maryland 20783, USA

qudsia.quraishi.civ@mail.mil

Abstract: The ability to filter unwanted light signals is critical to the operation of quantum memories based on neutral atom ensembles. Here we demonstrate an efficient frequency filter which uses a vapor cell filled with ^{85}Rb and a buffer gas to attenuate both residual laser light and noise photons by nearly two orders of magnitude with little loss to the single photons associated with our cold ^{87}Rb quantum memory. This simple, passive filter provides an additional 18 dB attenuation of our pump laser and erroneous spontaneous emissions for every 1 dB loss of the single photon signal. We show that the addition of a frequency filter increases the non-classical correlations and readout efficiency of our quantum memory by $\approx 35\%$.

1. Introduction

Distribution of entangled quantum states over significant distances is important to the development of future quantum technologies such as long-distance cryptography, networks of atomic clocks, distributed quantum computing, etc. [1, 2, 3, 4, 5]. Quantum repeaters can overcome the problems of exponential losses in direct transmission of single photons over quantum channels through entanglement swapping of remotely placed quantum memories via single photon detection [6]. Long-lived quantum memories and single photon sources are building blocks for systems capable of efficiently and securely transferring quantum information over extremely long distances. Quantum memories are a very active area of research with many different quantum systems as viable candidates, including ions [7], neutral atom ensembles [8], Rydberg atoms [9, 10, 11], single neutral atoms [12], quantum dots [13], and nitrogen vacancy centers [14]. Cold ensembles of neutral atoms are a favorable platform for quantum memories and single photon sources as they can store single excitations in long-lived ground states that lead to extremely long coherence times [15, 16].

The ability to store and retrieve single excitations efficiently and background-free is crucial to building quantum memories based on neutral atom ensembles [17]. The generation (retrieval) of these excitations usually requires a strong laser beam to create a coherent excitation in the atomic ensemble that can be heralded (read out) by the detection of a single photon from the ensemble. The detection of classical pump photons at the single photon detector is a source of error in standard quantum communication protocols that needs to be eliminated. This strong pump can be filtered by a variety of means: spatial, polarization, frequency, etc. Spatial filtering is achieved using the off-axis geometry pioneered in [18]. By aligning the single photon arms a few degrees off-axis from the pump arms, noise suppression > 40 dB is possible, usually limited by scattering off the surfaces near the memory. Polarization filtering is accomplished by post-selecting single photons that are orthogonally polarized to the corresponding pump

fields using properly aligned waveplates and polarizing optical elements. Birefringence of optical elements and imperfect polarizers usually limit noise suppression to ~ 40 dB as well [19]. Optical cavities [12], optically pumped atomic vapor cells [20], and fiber Bragg gratings [21] are just a few examples of frequency selective elements that have been used in various quantum memory experiments to reject sources of noise. It is possible to achieve extremely high levels of noise rejection (> 100 dB) though usually at the cost of lower transmission probability ($\approx 10\%$) [19]. Each of these frequency filters require complicated electronics, significant temperature stabilization, external references, or additional lasers.

In this paper, we show how the serendipitous near degeneracy of spectral lines in ^{85}Rb and ^{87}Rb allow one to construct an efficient frequency filter for both the classical pump beams and erroneous atomic decays in a neutral atom quantum memory, without strong filtering of the desired signal that herald the creation of these coherent excitations. To accomplish this we use the two naturally-occurring isotope of rubidium, ^{87}Rb for use as a quantum memory and a vapor cell filled with isotopically-pure ^{85}Rb to filter the pump photons associated with this process (Fig. 1). By properly choosing the correct transition in ^{87}Rb for the creation of spin-waves, the frequency of the Write beam and Noise single photons are nearly resonant with a transition in ^{85}Rb , while the single photons that are correlated to the created spin-waves are much further detuned from any transition in ^{85}Rb . The Noise single photons arise from spontaneous decays back to the original ground state ($5S_{1/2}, F = 2$). This method for filtering radiation is well known in the atomic clock community [22], and has been used in warm vapor quantum memory experiments previously [23, 24, 25]. A vapor cell frequency filter would be much more effective for a cold atom quantum memory because the Noise and Signal emissions from the cold ensemble are limited only by the atomic linewidth and not the much larger Doppler-broadened linewidth for warm vapor memories. A broader linewidth makes it more difficult to efficiently filter Noise processes while not absorbing the single photons heralding the creation of spin-waves needed for the operation of the quantum memory.

First, we build a simple model to predict the utility of such a filter under conditions that can be verified experimentally. Then, we perform an experiment where the filter is used to block spontaneously emitted photons not associated with the creation of spin-waves, which would contribute to a reduced readout efficiency. The result is a quantum memory with higher readout efficiency, hence higher single photon rates and greater nonclassical correlations.

2. Theory

To construct a frequency filter that is capable of attenuating the undesired background radiation it will be necessary to calculate the strength and the lineshape of the filter as a function of vapor cell temperature and buffer gas pressure. In the limit that the frequency of the input light is much more narrow-band (roughly the atomic linewidth $\Gamma/2\pi \approx 5.8$ MHz) than the bandwidth of the frequency filter ($\gg 100$ MHz) [26],

$$\frac{I_{OUT}(z)}{I_{IN}} = e^{-a(\delta, T, P)z} \quad (1)$$

where $a(\delta, T, P)$ is the attenuation per unit length that depends on the detuning from the nearest resonance line δ , temperature of the filter cell T , and buffer gas pressure P , while z is the length of the filter cell. The lineshape of the filter function may depend on both the inhomogeneous broadening due to the Doppler effect of atoms at a temperature T with a characteristic FWHM of $\delta v_D(T)$ and the homogeneous broadening due to collisions with a buffer gas at pressure P with a characteristic FWHM of $\gamma(P)$. The vapor cell filter is considered in two limits: when Doppler effects dominate and when atomic collisions dominate.

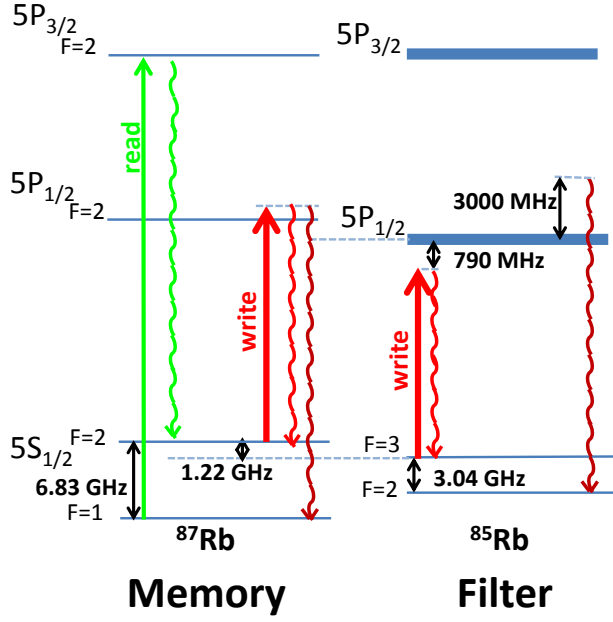


Fig. 1: The relevant energy levels and transitions of ^{87}Rb and ^{85}Rb used in this paper. The write beam is 20, 40, or 60 MHz blue-detuned from the $5S_{1/2}, F=2 \rightarrow 5P_{1/2}, F=2$ (D1) transition. Atoms excited to the $5P_{1/2}, F=2$ state can decay to either the $5S_{1/2}, F=1$ or the $5S_{1/2}, F=2$ ground state in ^{87}Rb . The write beam and the emission from the $5P_{1/2}, F=2 \rightarrow 5S_{1/2}, F=2$ state are detuned from the Doppler-broadened $5S_{1/2}, F=3 \rightarrow 5P_{1/2}$ transition in ^{85}Rb by ≈ 790 MHz. The emission from the $5P_{1/2}, F=2 \rightarrow 5S_{1/2}, F=1$ state is detuned from the Doppler-broadened $5S_{1/2}, F=2 \rightarrow 5P_{1/2}$ transition in ^{85}Rb by ≈ 3000 MHz. This difference in the detuning of these transitions serves as the basis for using a ^{85}Rb vapor cell as a frequency filter in our quantum memory experiment. The read beam is resonant with the $5S_{1/2}, F=1 \rightarrow 5P_{3/2}, F=2$ (D2) transition in ^{87}Rb . Drawing not to scale.

In the Doppler-broadened case:

$$a(T) = f(T) \exp\left[\frac{-4 \ln 2 \delta_i^2}{(\delta \nu_D(T))^2}\right] \quad (2)$$

where $f(T)$ is proportional to the vapor cell atom number and increases exponentially with cell temperature [27], $\delta \nu_D(T)$ is the Doppler-broadened FWHM of the ^{85}Rb lines, and δ_i is either the Noise or Signal frequency detuning from the nearest ^{85}Rb resonance shown in Fig. 1(a).

One would like a simple/passive frequency filter for strong attenuation of unwanted back-ground radiation with weak attenuation of the signal photons associated with the created spin waves. Figure 2(a) shows that an optically thick vapor cell of pure ^{85}Rb with no buffer gas would accomplish this due to the exponential falloff of the filter strength as a function of δ^2 and the detuning of the light associated with the desired transition is roughly four times further detuned than the light associated with the undesired transition (790 MHz vs 3000 MHz). However, contamination of the cell with a small amount ^{87}Rb can have a significant effect on the attenuation of the Signal photons. If the ratio of $^{87}\text{Rb}/^{85}\text{Rb}$ is on the order of a few times 10^{-3} (which is roughly the level of purification available commercially) this will result in roughly

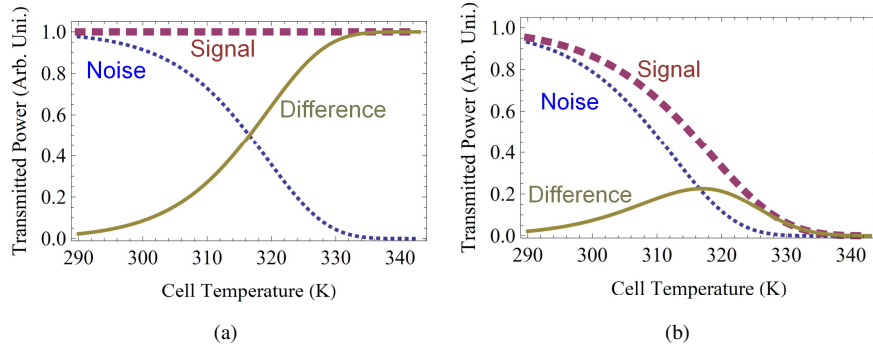


Fig. 2: Plots of the transmitted light through the vapor cell filter as a function of temperature in the Doppler-broadened limit (Eq. 2) for a filter cell length of 1 inch. **(a)** The pure ^{85}Rb filter cell acts nearly perfectly by attenuating the undesired light strongly (blue, dotted) and no attenuation of the signal (magenta, dashed) leading to large difference in attenuation between the two signals (gold, solid). **(b)** Small concentrations of ^{87}Rb ($^{87}\text{Rb}/^{85}\text{Rb}$ fraction of 0.2%) result in strong attenuation of the resonant background and signal fields. The emission from the cold ^{87}Rb ensemble is assumed to be hyperfine specific but the absorption by the warm ^{85}Rb vapor cell transitions are assumed to be Doppler-broadened and not hyperfine specific (See Fig. 1).

equal attenuation of the Noise photons by ^{85}Rb and Signal photons by ^{87}Rb , negating the utility of the frequency filter in Figure 2(b). It is therefore prudent to consider the frequency filter in the presence of a buffer gas to see if the effect of ^{87}Rb can be mitigated.

In the pressure-broadened case:

$$a(T, P) = f(T) \frac{\alpha P}{\pi(\delta_i - \beta P)^2 - (\frac{\alpha P}{2})^2} \quad (3)$$

where β is the coefficient for the linear frequency shift with a value of -6.7 MHz/Torr and α is the linear coefficient for the pressure-broadened linewidth with a value of 21 MHz/Torr at $T = 300 \text{ K}$ for the D1 transition due to collisions of Rb with an Argon buffer gas. Since we will only vary the temperature of the vapor cell by $\sim 10\%$ it will be a good approximation to say that these pressure-dependent coefficients are constant as a function of temperature. Figure 3 is a plot of Eq. 1 with $a(T, P)$ from Eq. 3 which shows how the introduction of 47 Torr of an Ar buffer gas changes the filter response as a function of vapor cell temperature. The Ar pressure of 47 Torr was chosen such that the filter could be modeled in the pressure-broadened limit ($\alpha P > \delta_{\nu_D}$) where the filter is most effective. Increasing the buffer gas pressure significantly would dilute the filter strength by broadening the filter response function. From Fig. 3 one can extract an 18 dB attenuation from the Noise for every 1 dB attenuation of the Signal over the range of filter cell temperatures measured. Disagreements between data and theory at higher filter cell temperatures may be explained by either violations of assumptions made in our simple model (such as temperature independent $\gamma(P)$) or greater ^{87}Rb contamination in the vapor cell than the specification from the manufacturer ($^{87}\text{Rb}/^{85}\text{Rb} \approx 0.2\%$).

The optimum operating temperature for the vapor cell filter should correspond to roughly the maximum difference between the Signal and Noise if one assumes roughly equal contributions of Signal and Noise before the frequency filter. This strikes a balance between increasing the Readout Efficiency and $g^{(2)}$ correlations (strong attenuation of Noise) while maximizing the

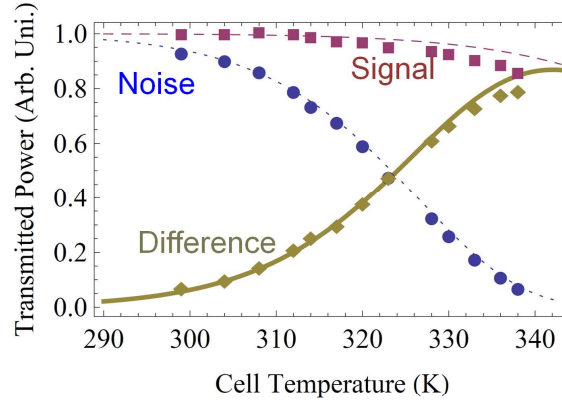


Fig. 3: Normalized measured transmission of classical laser light at the Noise (circles) and Signal (squares) frequencies and the difference between the two signals (diamonds) at a variety of vapor cell temperatures with 47 Torr of Ar in a 1 inch long ^{85}Rb vapor cell. The corresponding solid lines are calculations of the transmitted light through the vapor cell filter as a function of temperature with 47 Torr of Ar using the filter response from Eq. 3.

coincident count rate (weak attenuation of Signal). With a buffer gas of sufficient pressure and high enough operating temperature it is possible to achieve significant attenuation of the background light with only a small amount of signal loss.

3. Experimental Results and Methods

3.1. Neutral Atom Quantum Memory

A magneto-optical trap (MOT) of ^{87}Rb atoms produces an optically thick atomic ensemble for our experiment (Fig. 4(a)). Approximately 25 mW/cm^2 of cooling light, detuned 15 MHz below the $5S_{1/2}, F=2 \rightarrow 5P_{3/2}, F=3$ transition in ^{87}Rb , and 5 mW of repump light, on resonance with the $5S_{1/2}, F=1 \rightarrow 5P_{3/2}, F=2$ transition, are delivered collinearly to the vacuum system. Loading from a room-temperature Rb vapor, a cloud of $\sim 1.8 \times 10^8$ atoms at a temperature of $\sim 100 \mu\text{K}$ is produced in roughly 5 seconds with a magnetic field gradient of 10 G/cm (subsequent reloading of the MOT is performed in 30 ms as seen in Fig. 4(b)). This is then followed by a compressed MOT stage that consists of simultaneously lowering the intensity of the repump and increasing the gradient of the quadrupole magnetic field to 22 G/cm for 6 ms before turning the field off. The cooling light is turned off $100 \mu\text{s}$ later, and the repump light $2 \mu\text{s}$ after that, leaving all of the atoms in the $5S_{1/2}, F=2$ ground state.

A sequence of 1000 trials with individual durations of $\sim 1 \mu\text{s}$ is performed as follows: a weak, linearly-polarized, Write pulse, tuned 20, 40, or 60 MHz above the $5S_{1/2}, F=2 \rightarrow 5P_{1/2}, F=2$ (See Fig. 1) transition is shone on the atomic ensemble. The Write pulse has a $400 \mu\text{m}$ waist and 50 ns duration set by an acousto-optical modulator and an electro-optic modulator. For low enough excitation probability ($10^{-2} - 10^{-4}$) a photon detection within an 80 ns time interval at Si avalanche photodiode (APD) heralds the transfer of one ^{87}Rb atom in the ensemble from the $F=2$ ground state to the $F=1$ ground state in a particular spatial mode that has a waist of $200 \mu\text{m}$ at the MOT. From measurements of the atomic density, beam size, and length of the ensemble we can estimate that $\approx 10^6$ - 10^7 atoms participate in this process. The polarization of the generated single photon is post-selected to be orthogonal to the Write pulse with appropriate waveplates and linear polarizers. After a hold time of 200 ns, a strong, linearly-

polarized (orthogonal to the Write), resonant Read pulse of duration 300 ns and 400 μm waist interacts with the ensemble, producing a photon that is detected by APD B within a 100 ns window. The generated photon has a polarization orthogonal to the Read pulse. The single photon detection arms are aligned at an angle of 3° relative to the classical pump beams. By aligning the single photon arms a few degrees off-axis from the pump arms, the pump light is suppressed by a measured value of ≈ 40 dB in the single photon detection arms. The APD signals are sent to a time-interval analyzer (TIA) for data collection and analysis.

The strength of the correlations between the photon-pairs generated by the atomic ensemble can be measured by the normalized intensity cross-correlation function:

$$g_{A,B}^{(2)} = \frac{p_{AB}}{p_A p_B} = \frac{RE}{p_B} \quad (4)$$

where p_{AB} is the probability to detect a photon pair, p_i is the probability for an event click at detector i , and RE is the readout efficiency defined as p_{AB}/p_A . A plot of $g_{A,B}^{(2)}$ over a range of different write probabilities, p_A , is shown in Figure 4(c). Figure 4(c) shows a series of measurement of $g_{A,B}^{(2)}$ over a range of values for p_A ($10^{-2} - 10^{-4}$) with $\Delta_w/2\pi = 20$ MHz and a constant filter cell temperature of 336 K. The value of $g_{A,B}^{(2)}$ saturates at low p_A due to dark counts in the APDs and contamination of the readout arm by classical Read light. The transmission values for the Noise and Signal photons in Fig. 3 at a filter cell temperature of 336 K are 12% and 88% respectively. The filter cell attenuates the Noise photons significantly which increases the measured RE and $g_{A,B}^{(2)}$ for a given p_A while not significantly attenuating the Signal photons. Attenuation of the Signal photons would lead directly to a decrease in the coincidence probability, p_{AB} , an undesirable outcome for entanglement creation and entanglement swapping operations.

3.2. Filtering Single Photon Noise

In this section we study the effect of a ^{85}Rb filter on the operation of a cold ^{87}Rb quantum memory. This was done by varying the temperature of AR-coated vapor cell filled with isotopically-pure ^{85}Rb and 47 Torr of Argon from 298 K to 336 K. Based upon Fig. 3 we would expect the presence of ^{85}Rb vapor cell filter to have only a small effect on the quantum memory parameters (p_A , RE , $g_{A,B}^{(2)}$) at an operating temperature of 298 K. At this temperature the filter cell absorbs only 10% of the Noise photons and less than 1% of the Signal photons. However, as the filter cell temperature is increased, an increasing percentage of Noise photons (pump and emitted) are filtered by the cell with corresponding decreases in p_A and increases in RE and $g_{A,B}^{(2)}$. Fig. 5(a) shows the decrease in write probability as a function of filter cell temperature. For $\Delta_w/2\pi = 20$ MHz the Write probability decreases from a value of 6.5×10^{-4} to 5×10^{-4} as the filter cell temperature is increased from 298 K to 336 K. For Write detunings of 40 MHz and 60 MHz the Write probability decreases from 7×10^{-4} to 5×10^{-4} over the same temperature range. Most of this decrease can be attributed to the vapor cell filter absorption of Noise photons emitted by the cold ensemble taking into account the results of Fig. 3. At a filter cell temperature of 336 K only 6% of Noise photons are transmitted through the vapor cell while $> 85\%$ of Signal photons are transmitted. The vapor cell also filters out pump photons from the Write beam that scatter off of the vacuum system glass walls. However the effect on the quantum memory parameters is minimal because the pump contamination in the Write detection arm is only $\sim 1 \times 10^{-5}$. Since the filter cell has little effect on the coincident counts between detectors A and B, there is then a corresponding increase of $\approx 35\%$ in the measured Readout Efficiency as seen Fig. 5(b) for $\Delta_w/2\pi = 40$ and 60 MHz and $\approx 15\%$ for $\Delta_w/2\pi = 20$ MHz. Readout Efficiency increases from 6% to 7% for a Write detuning of 20 MHz, from 5.8% to 7.5% for a Write detuning of 40 MHz, and 5.5% to 7% for a Write detuning of 60 MHz.

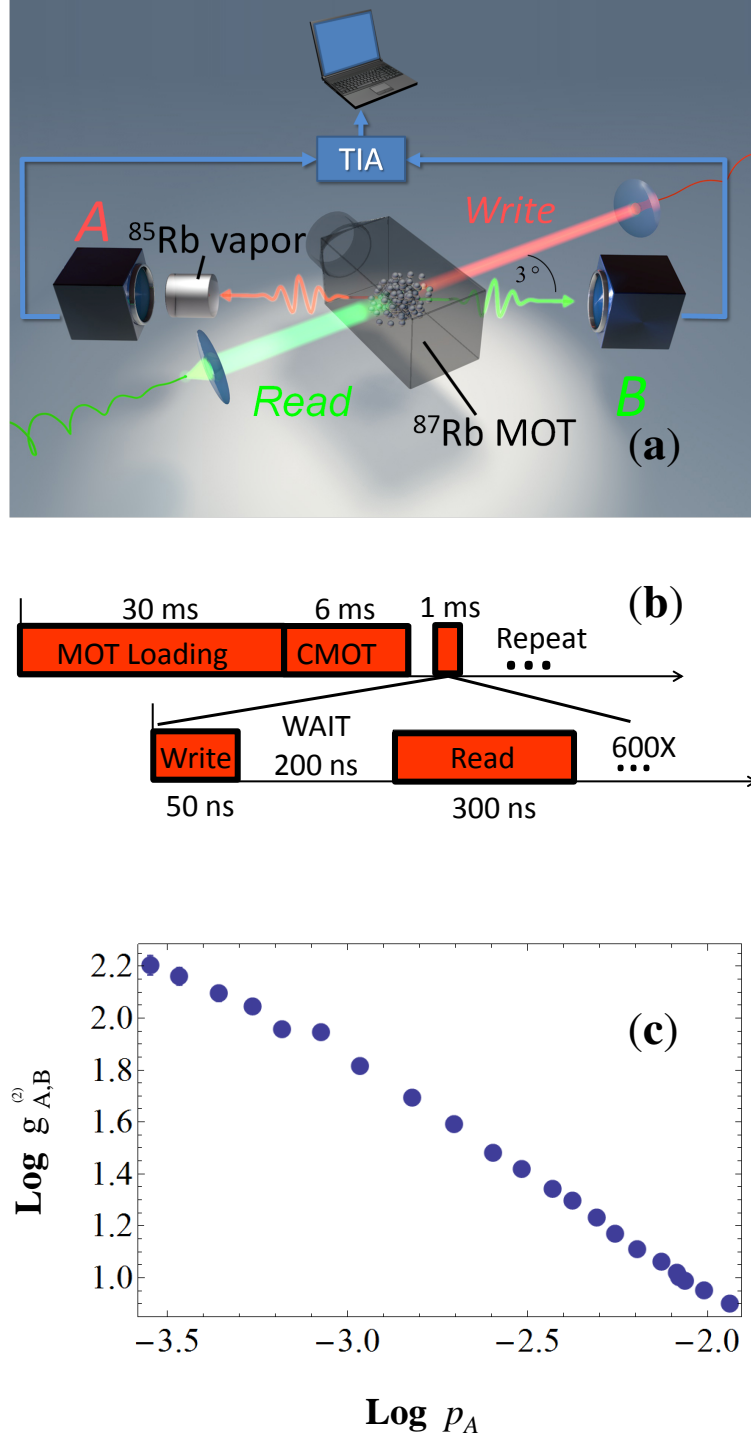


Fig. 4: **(a)** The experimental setup for our quantum memory. Counter-propagating Write and Read light pulses interact with a cold ^{87}Rb ensemble while emitted single photons are detected off-axis by Si APDs. Arrival times of the photons are measured by a time-interval analyzer (TIA) and sent to a PC for analysis. Emitted Write photons are filtered by a warm ^{85}Rb vapor cell to attenuate Noise photons. **(b)** Timing sequence for the production of a cold ensemble and interaction with Write and Read beams. A MOT is loaded and compressed to create a cold, dense atomic medium at a rate of 27 Hz. The MOT magnetic and laser fields are then extinguished for a 1 ms duration and a series of 600 Read-Write pulses interact with the system. **(c)** Log-Log plot of $g_{A,B}^{(2)}$ as a function of p_A with filter cell at a temperature of 336 K and $\Delta_w/2\pi = 20$ MHz. Write probability (p_A) is varied from $10^{-2} - 10^{-4}$ and the corresponding values of $g_{A,B}^{(2)}$ increase from ≈ 8 to > 160 .

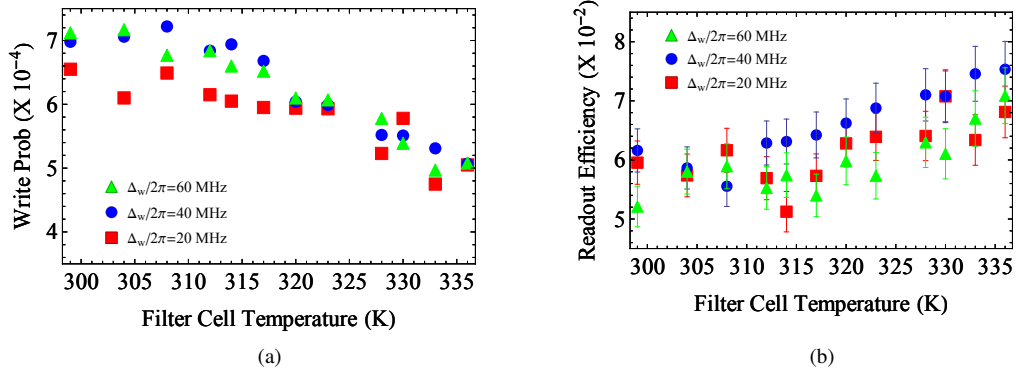


Fig. 5: Probability of detecting a write photon and Readout Efficiency as a function of the filter cell temperature for $\Delta_w/2\pi = 20, 40$, and 60 MHz. **(a)** The write probability decreases by $\approx 40\%$ over the range of filter cell temperatures used in this experiment for each write beam detuning. **(b)** A significant increase in Readout Efficiency as the filter cell temperature is increased is observed. The decrease in Noise photon detection in the Write arm leads to an $\approx 35\%$ increase in the Readout Efficiency for $\Delta_w/2\pi = 40$ and 60 MHz and $\approx 15\%$ for $\Delta_w/2\pi = 20$ MHz. Each point in plots (a) and (b) correspond to ~ 10000 write detection events and ~ 500 coincident counts respectively. The running time required to obtain a single data point is ≈ 12 minutes. Error bars are calculated assuming Poissonian statistics.

Any change in the Readout Efficiency due to the vapor cell filter necessarily should lead to a change in $g_{A,B}^{(2)}$ as the filter cell has no effect on p_B . Following the increases in RE seen in Fig. 5(b), a similar $\approx 35\%$ increase in the value of $g_{A,B}^{(2)}$ for $\Delta_w/2\pi = 40$ and 60 MHz is seen in Fig. 6 as the absolute values of $g_{A,B}^{(2)}$ increase from 95 to 130 and 100 to 135 respectively. For $\Delta_w/2\pi = 20$ MHz a smaller increase in $g_{A,B}^{(2)}$ of $\approx 15\%$ (from 95 to 110) corresponds closely to the similar increase of RE seen in Fig. 5(b) as well.

The difference in the performance of the vapor cell filter for the three write detunings can be partially explained by effective optical depth of the atomic ensemble at different Write beam detunings. Based upon $\Delta_w/2\pi = 20$ MHz (3.3Γ) and a measured $OD_{res} = 12$ for the atomic ensemble, one would expect an effective optical depth of the cloud for the created photons to be $OD_{3.3\Gamma} \approx 0.24$ from the equation: $OD_{\Delta} = OD_{res}(1 + (2\Delta/\Gamma)^2)^{-1}$ [28]. However that assumes the emitted single photons interact with the entire ensemble. The probability for excitation is proportional to the atomic density which is largest in the center of the ensemble. As a consequence, the average single photon would only see half the atoms in the cloud. The resulting OD (≈ 0.12) leads to $\approx 11\%$ attenuation of Noise single photons emitted by the ensemble. For the dataset with $\Delta_w/2\pi = 40$ (60) MHz there is only 3% (1%) attenuation of Noise single photons due to the smaller effective optical depth from the larger detuning. Since there are slightly more Noise photons for the larger Write detuning, the vapor cell has a relatively larger effect on the write probability, readout efficiency, and non-classical correlations for $\Delta_w/2\pi = 40$ and 60 MHz.

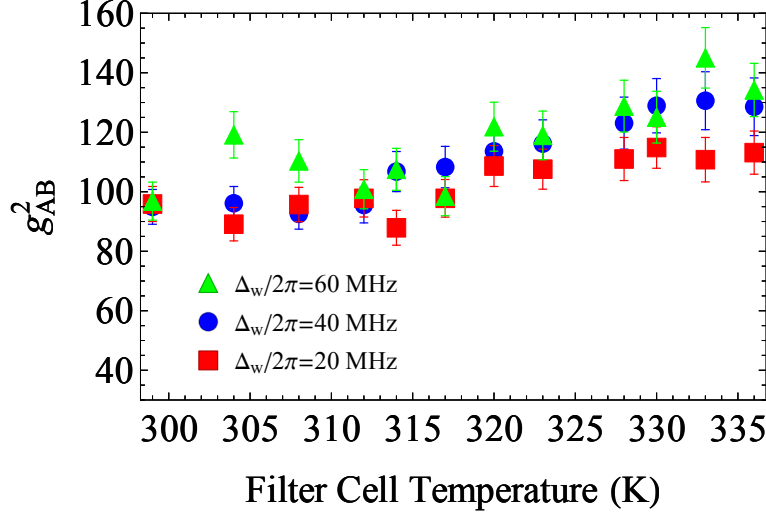


Fig. 6: $g_{A,B}^{(2)}$ correlations as a function of filter cell temperature for $\Delta_w/2\pi = 20, 40$ and 60 MHz. The strength of the correlations increase by $\approx 15\%$ for $\Delta_w/2\pi = 20$ MHz, $\approx 35\%$ for $\Delta_w/2\pi = 40$ MHz, and $\approx 35\%$ for $\Delta_w/2\pi = 40$ MHz. The increase in non-classical correlations follows directly from the increase in Readout Efficiency seen in Fig. 5. Error bars are calculated assuming Poissonian statistics.

4. Conclusions

In this paper we have shown how a temperature-controlled vapor cell filled with isotopically-pure ^{85}Rb filled with 47 Torr of Ar buffer gas increases the Readout efficiency and the non-classical correlations between the single photons emitted from the cold ^{87}Rb ensemble. The filter cell achieves a substantial reduction in the detection of Noise photons by frequency-selective absorption with little effect on the detection of Signal photons. Our model showed that a buffer gas in the vapor cell was required to eliminate the detrimental effect of the ^{87}Rb contamination in commercially available isotopically-pure ^{85}Rb vapor cells. Our experiments showed that for Write detunings of 40 and 60 MHz the measured Readout Efficiency and $g_{A,B}^{(2)}$ of our quantum memory increased by $\approx 35\%$ as the filter cell temperature was tuned from 298 K to 336 K due to the significant decrease in the detection of Noise photons. Less dramatic effects were seen for a Write detuning of 20 MHz which were partially explained by the detuning-dependent optical depth of the cold atomic ensemble. These results are important to maximizing the operating parameters that are critical to the realization of a quantum network based on neutral atom quantum memories.

Acknowledgments

We would like thank N. Solmeyer, D. Matsukevich, and A. Gorshkov for discussions on the quantum memory and P. Kunz for discussions on the vapor cell. DS is an Oak Ridge Associ-

ated Universities (ORAU) postdoctoral fellow. Research was sponsored by the Army Research Laboratory. The views and conclusions contained in this document are those of the Authors and should not be interpreted as representing the official policies, either expressed or implied, of the Army Research Laboratory or the U.S. Government. The U.S. Government is authorized to reproduce and distribute reprints for Government purposes notwithstanding any copyright notation herein.

References and links

1. C. H. Bennet and G. Brassard. Quantum cryptography: Public key distribution, and coin-tossing. *Proc. 1984 IEEE International Conference on Computers, Systems, and Signal Processing*, pages 175–179, 1984.
2. Nicolas Gisin, Grgoire Ribordy, Wolfgang Tittel, and Hugo Zbinden. Quantum cryptography. *Reviews of modern physics*, 74(1):145–195, 2002.
3. H. J. Kimble. The quantum internet. *Nature*, 453(7198):1023–1030, June 2008.
4. Michael A Nielsen and Chuang, Isaac L. *Quantum computation and quantum information*. Cambridge University Press, Cambridge [u.a.], 2013.
5. P. Komr, E. M. Kessler, M. Bishof, L. Jiang, A. S. Srensen, J. Ye, and M. D. Lukin. A quantum network of clocks. *Nature Physics*, 10(8):582–587, August 2014.
6. H.-J. Briegel, W. Dr, J. I. Cirac, and P. Zoller. Quantum repeaters: The role of imperfect local operations in quantum communication. *Physical Review Letters*, 81(26):5932–5935, December 1998.
7. S. Olmschenk, D. Hayes, D. N. Matsukevich, P. Maunz, D. L. Moehring, and C. Monroe. Quantum Logic Between Distant Trapped Ions. *International Journal of Quantum Information*, 08(01n02):337–394, February 2010.
8. D. N. Matsukevich and A. Kuzmich. Quantum state transfer between matter and light. *Science*, 306(5696):663–666, October 2004.
9. T. Wilk, A. Gatan, C. Evellin, J. Wolters, Y. Miroshnychenko, P. Grangier, and A. Browaeys. Entanglement of two individual neutral atoms using rydberg blockade. *Physical Review Letters*, 104(1):010502, January 2010.
10. L. Li, Y. O. Dudin, and A. Kuzmich. Entanglement between light and an optical atomic excitation. *Nature*, 498(7455):466–469, June 2013.
11. Bo Zhao, Markus Mller, Klemens Hammerer, and Peter Zoller. Efficient quantum repeater based on deterministic rydberg gates. *Physical Review A*, 81(5), May 2010.
12. Christian Nlleke, Andreas Neuzner, Andreas Reiserer, Carolin Hahn, Gerhard Rempe, and Stephan Ritter. Efficient teleportation between remote single-atom quantum memories. *Physical Review Letters*, 110(14), April 2013.
13. Miro Kroutvar, Yann Ducommun, Dominik Heiss, Max Bichler, Dieter Schuh, Gerhard Abstreiter, and Jonathan J. Finley. Optically programmable electron spin memory using semiconductor quantum dots. *Nature*, 432(7013):81–84, November 2004.
14. K. C. Lee, M. R. Sprague, B. J. Sussman, J. Nunn, N. K. Langford, X.-M. Jin, T. Champion, P. Michelberger, K. F. Reim, D. England, D. Jaksch, and I. A. Walmsley. Entangling macroscopic diamonds at room temperature. *Science*, 334(6060):1253–1256, December 2011.
15. A. Kuzmich, W. P. Bowen, A. D. Boozer, A. Boca, C. W. Chou, L.-M. Duan, and H. J. Kimble. Generation of nonclassical photon pairs for scalable quantum communication with atomic ensembles. *Nature*, 423(6941):731–734, June 2003.
16. Y. O. Dudin, L. Li, and A. Kuzmich. Light storage on the time scale of a minute. *Physical Review A*, 87(3):031801, March 2013.
17. L.-M. Duan, M. D. Lukin, J. I. Cirac, and P. Zoller. Long-distance quantum communication with atomic ensembles and linear optics. *Nature*, 414(6862):413–418, November 2001.
18. Danielle Braje, Vlatko Bali, Sunil Goda, G. Yin, and S. Harris. Frequency mixing using electromagnetically induced transparency in cold atoms. *Physical Review Letters*, 93(18), October 2004.
19. Connor Kupchak, Thomas Mittiga, Bertus Jordaen, Mehdi Namazi, Christian Nlleke, and Eden Figueroa. Room-temperature quantum memory for polarization states. *arXiv:1405.6117 [quant-ph]*, May 2014.
20. Julien Laurat, Hugues de Riedmatten, Daniel Felinto, Chin-Wen Chou, Erik W. Schomburg, and H. Jeff Kimble. Efficient retrieval of a single excitation stored in an atomic ensemble. *Optics Express*, 14(15):6912–6918, July 2006.
21. Xavier Fernandez-Gonzalvo, Giacomo Corrielli, Boris Albrecht, Marcel.li Grima, Matteo Cristiani, and Hugues de Riedmatten. Quantum frequency conversion of quantum memory compatible photons to telecommunication wavelengths. *Optics Express*, 21(17):19473–19487, August 2013.
22. James Camparo. The rubidium atomic clock and basic research. *Physics Today*, 60(11):33–39, November 2007.
23. Alexander Heifetz, Ashish Agarwal, George C. Cardoso, Venkatesh Gopal, Prem Kumar, and M.S. Shahriar. Super efficient absorption filter for quantum memory using atomic ensembles in a vapor. *Optics Communications*, 232(1-6):289–293, March 2004.

24. Stephanie Manz, Thomas Fernholz, Jrg Schmiedmayer, and Jian-Wei Pan. Collisional decoherence during writing and reading quantum states. *Physical Review A*, 75(4), April 2007.
 25. Mark Bashkansky, Fredrik K. Fatemi, and Igor Vurgaftman. Quantum memory in warm rubidium vapor with buffer gas. *Optics Letters*, 37(2):142–144, 2012.
 26. Peter W. Milonni and Joseph H. Eberly. *Laser Physics*. John Wiley & Sons, April 2010.
 27. Daniel A Steck. Rubidium 87 d line data, 2001.
 28. B M Sparkes, J. Bernu, M. Hosseini, J. Geng, Q. Glorieux, P. A. Altin, P. K. Lam, N. P. Robins, and B. C. Buchler. Gradient echo memory in an ultra-high optical depth cold atomic ensemble. *New Journal of Physics*, 15(8):085027, 2013.
-